ADVANCES IN ATMOSPHERIC SCIENCES, VOL. 32, JUNE 2015, 877–888

Characterization of Organic Aerosols in Beijing Using an Aerodyne High-Resolution Aerosol Mass Spectrometer

ZHANG Junke, WANG Yuesi, HUANG Xiaojuan, LIU Zirui, JI Dongsheng, and SUN Yang*

State Key Laboratory of Atmospheric Boundary Layer Physics and Atmospheric Chemistry, Institute of Atmospheric Physics, Chinese Academy of Sciences, Beijing 100029

(Received 10 July 2014; revised 18 October 2014; accepted 24 October 2014)

ABSTRACT

Fine particle of organic aerosol (OA), mostly arising from pollution, are abundant in Beijing. To achieve a better understanding of the difference in OA in summer and autumn, a high-resolution time-of-flight aerosol mass spectrometer (HR-ToF-AMS, Aerodyne Research Inc., USA) was deployed in urban Beijing in August and October 2012. The mean OA mass concentration in autumn was 30 ± 30 μg m^{-3}, which was higher than in summer (13 ± 6.9 μg m^{-3}). The elemental analysis found that OA was more aged in summer (oxygen-to-carbon (O/C) ratios were 0.41 and 0.32 for summer and autumn, respectively). Positive matrix factorization (PMF) analysis identified three and five components in summer and autumn, respectively. In summer, an oxygenated OA (OOA), a cooking-emission-related OA (COA), and a hydrocarbon-like OA (HOA) were indentified. Meanwhile, the OOA was separated into LV-OOA (low-volatility OOA) and SV-OOA (semi-volatile OOA); and in autumn, a nitrogen-containing OA (NOA) was also found. The SOA (secondary OA) was always the most important OA component, accounting for 55% of the OA in the two seasons. Back trajectory clustering analysis found that the origin of the air masses was more complex in summer. Southerly air masses in both seasons were associated with the highest OA loading, while northerly air masses were associated with the lowest OA loading. A preliminary study of OA components, especially the POA (primary OA), in different periods found that the HOA and COA all decreased during the National Day holiday period, and HOA decreased at weekends compared with weekdays.

Key words: organic aerosol, aerosol mass spectrometer, positive matrix factorization, seasonal difference

Citation: Zhang, J. K., Y. S. Wang, X. J. Huang, Z. R. Liu, D. S. Ji, and Y. Sun, 2015: Characterization of organic aerosols in Beijing using an aerodyne high-resolution aerosol mass spectrometer. *Adv. Atmos. Sci.*, **32**(6), 877–888, doi: 10.1007/s00376-014-4153-9.

1. Introduction

Organic aerosol (OA) is a primary contributor of fine particle pollution, constituting 20%–90% of the submicron particulate mass (Zhang et al., 2007). Meanwhile, OA greatly impacts the radiative budget of the Earth's atmosphere, in addition to reducing visibility, and harming human health (Alam et al., 2011). Therefore, a thorough understanding of the OA characteristics, sources, and the processes it undergoes in the atmosphere are very important for addressing aerosol-related pollution issues, and for the improvement of the predictive capability of air quality and climate models (Zhang et al., 2011).

Most previous aerosol studies have been based on filter sampling, followed by laboratory analysis. However, these methods usually have a lower resolution and cannot capture the dynamic changes of aerosol chemical composition and size distributions that occur over faster timescales than the sampling interval (Ulbrich et al., 2012). Over the past decade, high-resolution time-of-flight aerosol mass spectrometer (HR-ToF-AMS) instruments, particularly the commercial instruments made by Aerodyne Research Inc., have been widely used to study fine particulate matter. This has allowed detailed investigation of aerosol sources and processes.

Beijing, the political and cultural center of China, has developed rapidly in recent years: it is now one of the top ten polluted cities in the world (Yu et al., 2011). As expected, with the fast growth of the population and the number of motor vehicles, the air quality in Beijing has severely deteriorated. Fine particles are a top pollutant. OA in Beijing accounts for 30%–50% of the total particulate mass of PM_1 (particulate matter with an aerodynamic diameter <1 μm) (He et al., 2006), and therefore makes a strong contribution to the air pollution. Only a small number of reports have focused on OA in submicron particles in Beijing, measured by AMS. Sun et al. (2010) first used a quadrupole-based aerosol mass spectrometer (Q-AMS) to study non-refractory submicron particles (NR-PM_1) in Beijing in summer 2006.

* Corresponding author: SUN Yang
Email: suny@mail.iap.ac.cn

Three OA components were determined: hydrocarbon-like OA (HOA), and two oxygenated OA (OOA) components. Huang et al. (2010) first deployed a HR-ToF-AMS in Beijing and measured the chemical composition and size distribution of the detected submicron particles. The OAs were divided into two oxygenated organic aerosol types (OOA-1 and OOA-2), hydrocarbon-like (HOA), and cooking-related (COA). In January 2013, Beijing experienced several serious haze events, and during this time Zhang et al. (2014) deployed an Aerodyne HR-ToF-AMS to measure the NR-PM_1, and elucidated several factors for the pollution events based on the measurement results. Sun et al. (2013) found that aerosol composition, processes and sources vary between summer and winter, caused by seasonally dependent meteorology and source emissions. Therefore, knowledge of the seasonal variation of OA is relevant to effectively reduce air pollution in Beijing. However, there remains no high resolution autumn OA data, and seasonal differences have rarely been reported in Beijing (Sun et al., 2013; Zhang et al., 2013).

To achieve an in-depth understanding of OA in summer and autumn, and to analyze OA chemical characteristics, processes and sources, a high-resolution time-of-flight aerosol mass spectrometer (HR-ToF-AMS, Aerodyne Research Inc., USA) was deployed in Beijing in August and October 2012. The instrument was used to determine and compare the concentrations, size distributions, and extent of oxidation of the OA in summer and autumn. Additionally, the OA components were determined by positive matrix factorization (PMF) analysis of the high-resolution AMS data (PMF-AMS). Finally, the effects of air mass transport and human activities on the OA loading and OA components were analyzed. We must note that the AMS measurement results includes OA and other inorganic species (nitrate, sulfate, ammonium and chloride). In this study, we only focused on the OA and other inorganic species were only used to compare with the PMF results.

2. Methods and materials

2.1. *Sampling site description*

The HR-ToF-AMS was placed in the location used by Zhang et al. (2014), at the Institute of Atmospheric Physics (IAP), Chinese Academy of Sciences (CAS), in August (1 to 31 August) and October (1 to 31 October) 2012, to measure in real-time the size distributions and chemical compositions of ambient OA (Fig. S1). Meteorological parameters including temperature, humidity, and wind speed and direction were recorded by an automatic meteorological observation instrument (Milos520, Vaisala, Finland). Concentrations of NO and NO_2 as combined NO_x were measured using a chemiluminescence analyzer (Model 42i, Thermo-Fisher Scientific, USA). Data were collected every 5 minutes. Ambient air for AMS observation sampled 15 m above ground, while meteorological parameters and NO_x were sampled 8 m above ground.

2.2. *HR-ToF-AMS operation*

Full details of the HR-ToF-AMS instrument were published by DeCarlo et al. (2006). The operation of the HR-ToF-AMS during the campaign followed that of Zhang et al. (2014). The V- and W-ion optical modes were alternated every 7.5 minutes. In V-mode operation, the HR-ToF-AMS cycled through the mass spectrum (MS) and the particle time-of-flight (PToF) modes every 45 s, spending 22.5 s in open and closed status under MS mode, respectively. The size distribution data are reported in terms of particle vacuum–aerodynamic diameter. At the beginning, middle and end of the two seasonal study periods, the ionization efficiency (IE), inlet flow, and particle sizing were calibrated following standard protocols (Jimenez et al., 2003; Drewnick et al., 2005). The 7.5 minutes OA detection limit (DL) was determined to be 0.056 $\mu g\ m^{-3}$, three times the standard deviation of the signal in particle-free air.

2.3. *HR-ToF-AMS data analysis*

The analysis of the HR-ToF-AMS data was based on the standard analysis software packages SQUIRREL, version 1.50, and PIKA, version 1.09. A collection efficiency (CE) factor of 0.5 was used in this study. A detailed discussion on the choice of the CE is presented in supporting information (Part 1, Figs. S2 and S3). The relative ionization efficiency (RIE) value of organics used in this study was 1.4 (Canagaratna et al., 2007).

PMF analyses were performed on the HR-MS data using the PMF Evaluation Toolkit (PET), version v2.05 (Paatero and Tapper, 1994; Ulbrich et al., 2009). Data and error matrices were first generated in PIKA. Further information about the PMF analysis can be found in other related publications (e.g., Paatero and Tapper, 1994; Paatero and Hopke, 2003; Ulbrich et al., 2009; Huang et al., 2010; Zhang et al., 2014).

The PMF analyses in the two study seasons were performed for 1 to 8 factors. A detailed discussion of the optimal solutions choice is detailed in supporting information (Part2, Fig. S4). The 3 factor and the 5 factor were chosen as the optimal solutions in summer and autumn, respectively.

3. Results and discussion

3.1. *Mass concentrations and temporal variations of OA*

Figures S5 and S6 present the meteorological factors during the two seasons as hourly averaged values. The average ambient temperature and relative humidity in summer were $27^{\circ}C \pm 3.8^{\circ}C$ and $61\% \pm 18\%$, respectively. Wind speed varied from 0.0 to 3.5 m s^{-1}, with an average of 0.9 ± 0.7 m s^{-1}. As expected, the average ambient temperature and relative humidity were both decreased in autumn: they were $14^{\circ}C \pm 4.7^{\circ}C$ and $52\% \pm 20\%$, respectively. Meanwhile, the wind speed had a broader range, from 0.0 to 8.0 m s^{-1}, with a higher average of 1.2 ± 1.2 m s^{-1}.

The OA mass concentration time series had very different characteristics in summer and autumn. It was more stable in summer, with an OA mass concentration lower than 50

μg m^{-3}. The OA mass concentration varied greatly in autumn, often exceeding 100 μg m^{-3} (Fig. 1), with a broad range from 1.1 to 173 μg m^{-3}. The summer distribution had a range of was 0.96 to 46 μg m^{-3}. The mean mass concentrations of OA in summer and autumn were 13 ± 6.9 μg m^{-3} and 30 ± 30 μg m^{-3}, respectively. The summer value was much lower than that measured in Beijing in 2006 (28.1 μg m^{-3}) by Sun et al. (2010), and in 2008 (23.9 μg m^{-3}) by Huang et al. (2010). However, it was higher than the summer results of Huang et al. (2012) in Shanghai. The PM_1 mean mass concentration measured by Huang et al. (2012) was 29.2 μg m^{-3}, and the OA mass concentration was 8.4 μg m^{-3}. In addition, our summer OA value was also higher than those measured in other cities during the same season; e.g. 6.6 μg m^{-3} in Zurich, 6.3 μg m^{-3} in New York, and 2.2 μg m^{-3} in Pairs (Lanz et al., 2007; Sun et al., 2011; Crippa et al., 2013, respectively). The difference in the mean mass concentration of OA between Beijing and other major cities in China in autumn was also significant. The OA loading was only 18 μg m^{-3} in the Hong Kong-Shenzhen metropolitan area (He et al., 2011). These observations suggest that although the summer OA in Beijing has decreased significantly in recent years, it is still at a higher level compared with Shanghai or other foreign cities as we mentioned above. OA pollution in autumn remains elevated in Beijing.

The mean diurnal variations of OA during both seasons are presented in Fig. 2a. The OA were characterized by two peaks, which occurred at around noon (1100–1300 LST) and in the evening (1800–2300 LST). Such diurnal variations have often been observed in AMS measurements (Huang et al., 2010; Sun et al., 2011; Huang et al., 2012). However, measurements made in Pittsburgh by Zhang et al. (2005a) had a first peak corresponding to the morning rush hour during 0700-0900 LST which reflects the importance of traffic emissions (Zhang et al., 2005a). The concentration difference between the two peaks was much larger in autumn (35 μg m^{-3}) than in summer (6 μg m^{-3}). A smaller difference in summer was also observed in Shanghai (Huang et al., 2012). Meanwhile, the large difference in autumn was also measured in Shenzhen (He et al., 2011). The large difference between the two peaks appearing in autumn is likely a result of the significantly reduced nighttime mixing layer height. This effect was weak in summer due to the higher ambient temperature throughout the day and night. This is illustrated in Figs. S5 and S6: the lowest temperature in summer was about 17°C, while the lowest temperature in autumn was close to 0°C. In addition, the mean temperature in summer was 13°C higher than in autumn. The more detailed information about the difference of mixing layer height in different months in Beijing was discussed by He and Mao (2005) and You et al. (2010). The identification and discussion of different OA factors is presented in section 3.2.

Size distributions provide important information to understand aerosol sources, formation, and growth mechanisms (Lan et al., 2011). Figure 2b presents the average size distributions of OA determined by the HR-ToF-AMS during the two seasons. Although there was a large difference in OA concentrations, the OA all showed very similar size distributions. The peak for both distributions appeared at ∼600 nm, indicative of aged regional aerosols (Zhang et al., 2005b). Moreover, there was another smaller peak at ∼200 nm, which may be attributed to "fresh" combustion emissions (Sun et al., 2011). A similar phenomenon has been observed at other urban sites (Huang et al., 2011; Sun et al., 2010) and in chamber studies (Asa-Awuku et al., 2009).

The elemental composition is one of the most important physicochemical properties of OA. It can influence the density, hygroscopicity, and vapor pressure of the OA (Pang et al., 2006). The oxygen-to-carbon (O/C) atomic ratio is a good parameter for measuring the extent of oxidation of OA (Jimenez et al., 2009). In addition, the organic-mass-to-organic-carbon (OM/OC) mass ratio was used as a conversion factor, following the form of traditional filter-based aerosol chemistry studies. In summer, the mean value of the O/C and OM/OC mass ratios were 0.41 ± 0.10 and 1.70 ± 0.13; and they decreased in autumn, to 0.32 ± 0.11 and 1.59 ± 0.20, respectively. This difference indicates that the OA in summer was more aged than that in the autumn. This may result from higher temperatures and solar radiation during the summer months, which can enhance the OA aging and the increase of O/C ratio.

As shown in Fig. 3, the O/C and OM/OC mass ratios had high values in the afternoon (1500–1600 LST) and low values in the evening (after 1900 LST). This is because photochemi-

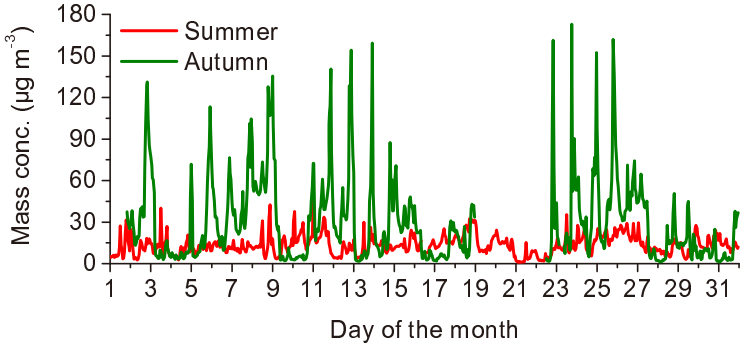

Fig. 1. Time series of the mass concentration of OA in summer and autumn.

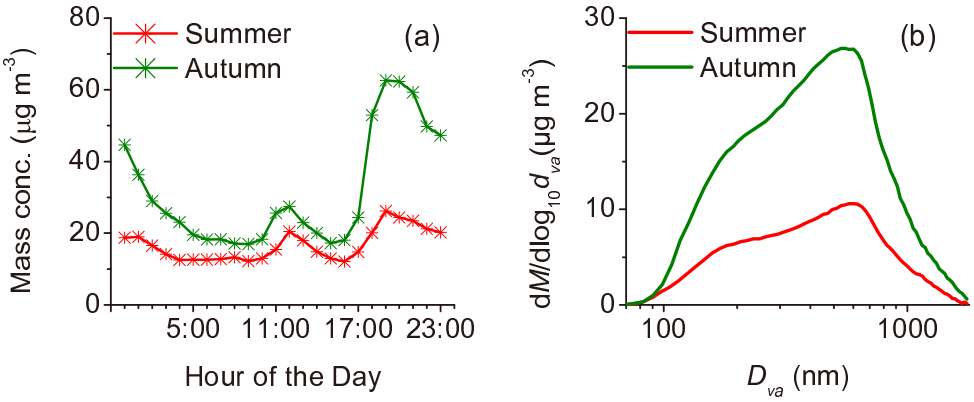

Fig. 2. The (a) diurnal cycle and (b) size distribution of OA during summer and autumn.

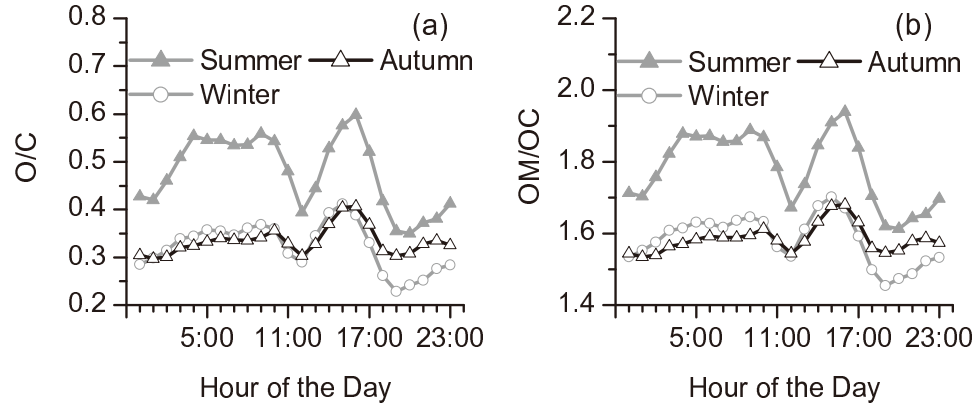

Fig. 3. The diurnal cycles of the O/C (molar ratio) and OM/OC (mass ratio) in different seasons.

cal reactions were most active in the afternoon, leading to the production of SOA with high O/C ratios. However, the minimum values of O/C and OM/OC occurred at 1200 LST and 1900 LST corresponding to the lunch time and evening meal and rush hours in Beijing. These findings reflect the fact that catering activities are an important factor affecting the oxidization of OA in Beijing. Ratios measured during winter campaigns by Zhang et al. (2014) were added to Fig. 3 for better comparison. Although the diurnal variation was similar during the different seasons, the ratios were significantly higher in summer than during autumn and winter.

3.2. *Investigating OA components/sources with PMF*

The PMF analysis identified three organic components present in the summer: oxygenated OA (OOA), cooking-related OA (COA), and hydrocarbon-like OA (HOA); and five present in the autumn: low-volatility oxygenated (LV-OOA) and semi-volatile oxygenated (SV-OOA), nitrogen-containing OA (NOA), COA, and HOA. Figures 4 to 7 show the MS profiles of every component and the time series of the OA factors and their relevant species in summer and autumn.

Generally, LV-OOA and SV-OOA were dominated by SOA. They had different O/C ratios and volatilities: LV-OOA, more oxidized and aged, has a higher O/C ratios, whereas SV-OOA, often less oxidized and fresher, has a lower O/C ratio (Jimenez et al., 2009). The MS of both OOA components were dominated by abundant $C_xH_yO_z^+$ fragments, especially by CO_2^+ (m/z 44), suggesting that oxidized organic compounds were present in large amounts (Figs. 4a, 6a and b). SV-OOA displayed a higher m/z 43 value (mainly $C_2H_3O^+$) than LV-OOA (Sun et al., 2011). However, the OOA could not be divided into LV-OOA and SV-OOA in summer in Beijing (Fig. 4a). The MS of OOA in summer was very close to the LV-OOA in autumn, with O/C ratios even higher than the LV-OOA (0.87 for OOA and 0.81 for LV-OOA).

The time series of OOA in summer and LV-OOA in autumn showed similar trends to that of sulfate ($R^2 = 0.77$ and 0.86, Figs. 5a and 7a). However, the correlation of SV-OOA in autumn with nitrate ($R^2 = 0.35$) was not as strong as that with other components, because nitrate can be generated not only through photochemical oxidation in daytime but also through the reaction of H_2O in particles and the decomposition of N_2O_5 at night. LV-OOA and OOA displayed similar diurnal cycles, characterized by a gradual increase in the daytime, with a maximum at noon. This reflects the dominant contribution from photochemical production in the daytime (Fig. 8a). The diurnal cycle of SV-OOA in autumn showed a lower value in the afternoon, likely due to higher ambient temperatures favoring the evaporation of semi-volatile

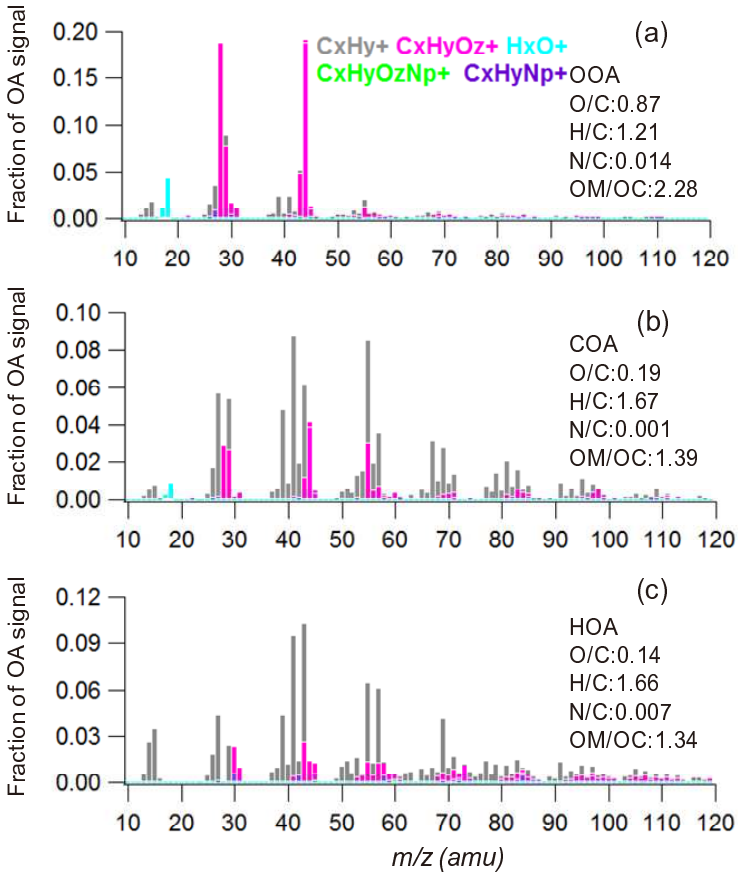

Fig. 4. The summer mass spectra of the (a) OOA, (b) COA, and (c) HOA components.

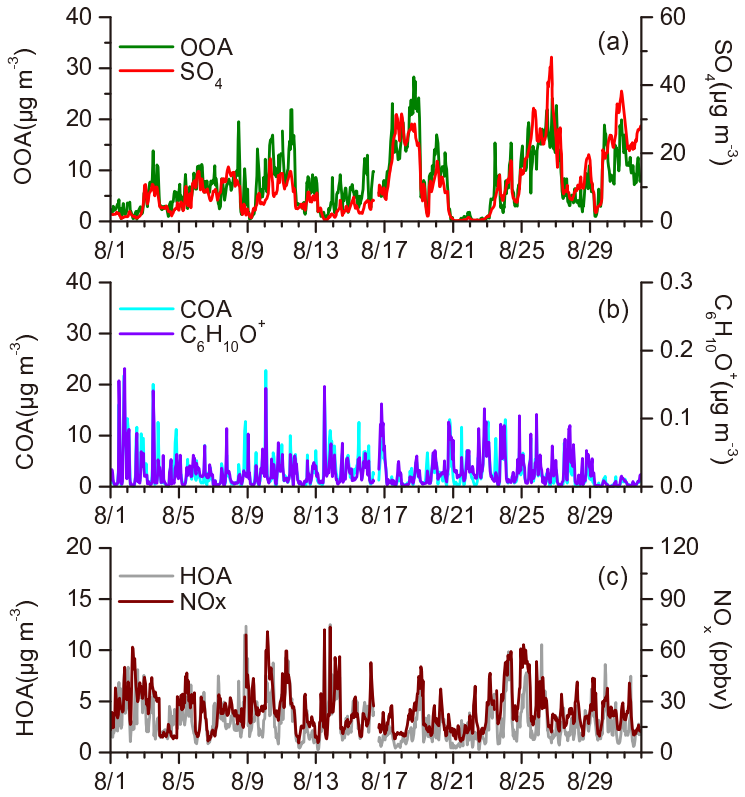

Fig. 5. The time series of three OA components and other relevant species in summer.

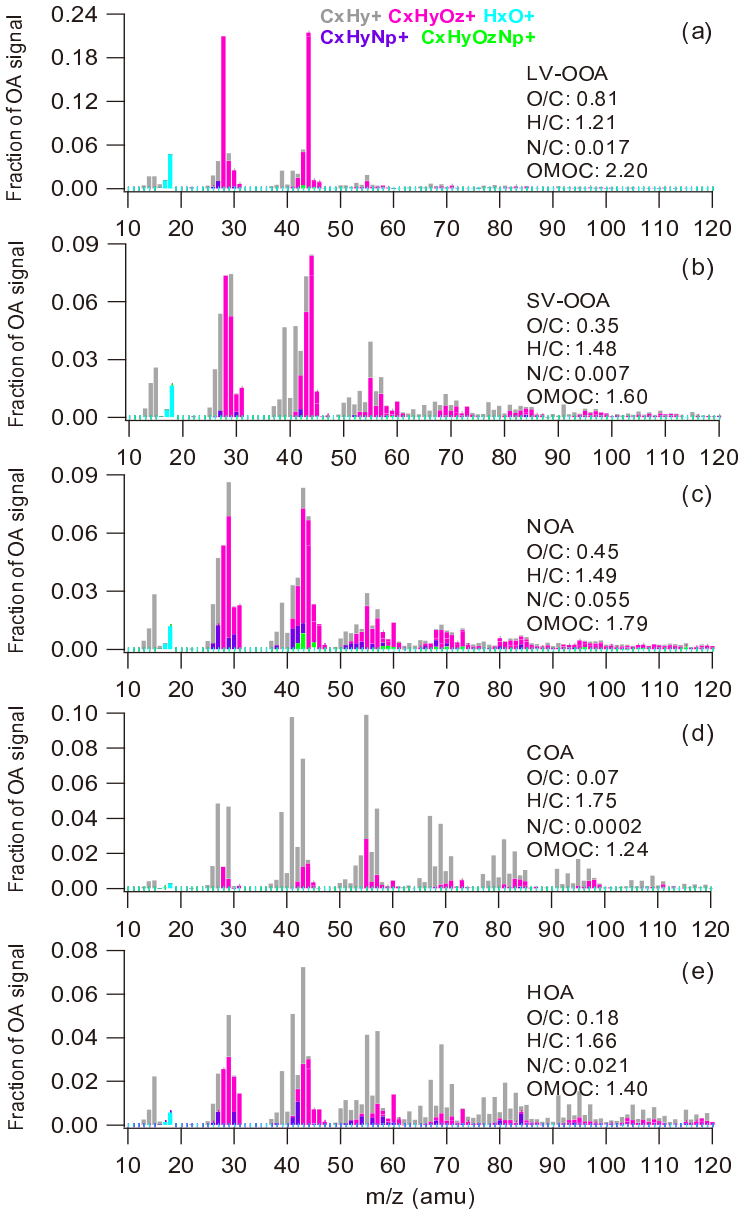

Fig. 6. The autumn mass spectra of the (a) LV-OOA, (b) SV-OOA, (c) NOA, (d) COA, and (e) HOA components.

species, which counteracted the photochemical production of SOA (Fig. 8a). As the decrease of SV-OOA was accompanied by a gradual increase of LV-OOA, further oxidation of more volatile and less oxidized species (i.e. SV-OOA) to less volatile and highly oxidized species (i.e. LV-OOA) occurred. LV-OOA and SV-OOA in autumn comprised 34% and 21% of the OA, respectively (Fig. 8b). Together, the OOAs accounted for 55% of the OA, similar to the contribution of OOA in summer (55%). These contributions from OOA during this study were consistent with previous findings in Barcelona (55%) (Mohr et al., 2012) and in Beijing (58%) (Huang et al., 2010; Zhang et al., 2013).

The third factor in autumn was identified as NOA, which exhibited the highest N/C ratio (0.055). This component accounted for 9% of the total organic mass (Fig. 8b). The highest nitrogen-containing fragments were at m/z 27 (CHN^+), m/z 29 (CH_3N^+), m/z 30 (CH_4N^+), m/z 41 ($C_2H_3N^+$) and m/z 42 ($C_2H_4N^+$) (Fig. 6c). This MS characteristic was very similar to that measured in the Po Valley (Saarikoski et al., 2012). A good correlation was reported between NOA and the N-containing $C_3H_8N^+$ ions ($R^2 = 0.57$). Similar OA component finding were also recorded in Mexico City (Aiken et al., 2009), with a N/C of 0.06. The mass spectrum of NOA also closely resembled that of OOA in our study. Sun et al. (2011) found that the NOA component was associated with atmospheric amines. Meanwhile, Ge et al. (2011) performed a detailed review of the sources of atmospheric amines, identifying many anthropogenic and natural sources. They found

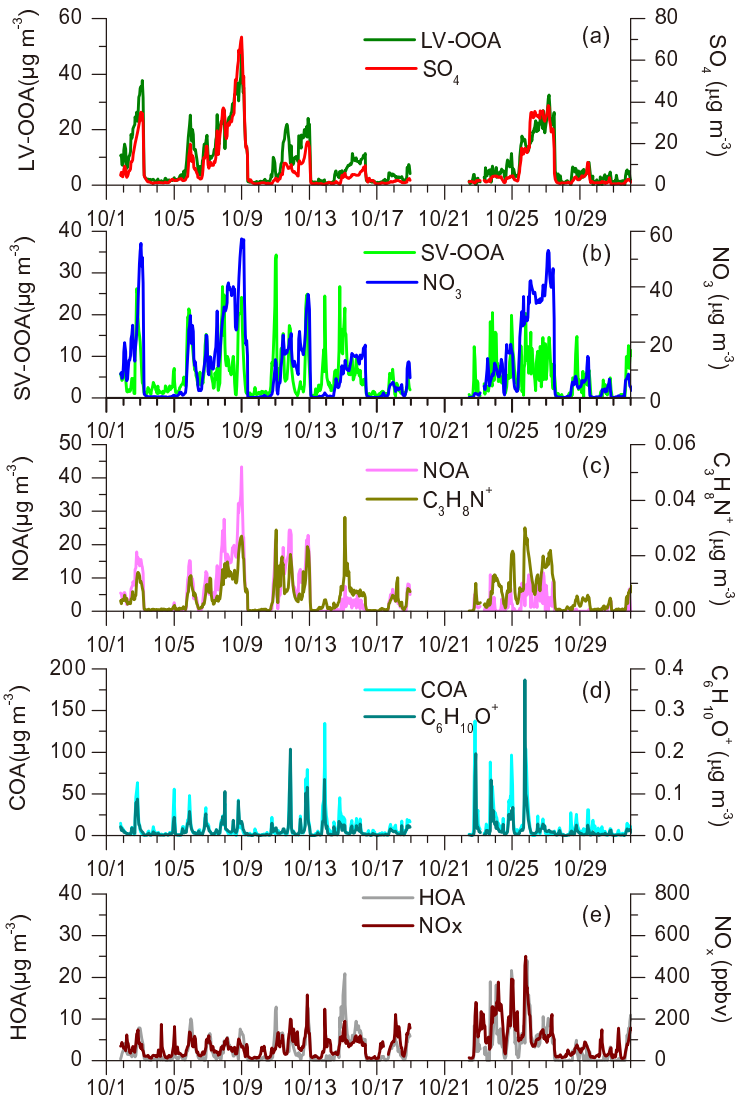

Fig. 7. The time series of five OA components and other relevant species in autumn.

that biomass burning was a primary source of many trace substances, and C_1 to C_5 (the number of C atom from 1 to 5) amines were produced during the burning process. Meanwhile, biomass burning may also release some long-chain alkyl amides. Accordingly, we found a prominent contribution of m/z (mass to charge) 60 in the NOA MS in our study: a good tracer for biomass burning (Aiken et al., 2009). Therefore, this OA component likely came from biomass burning. However, the NOA was only identified during the autumn sampling period, as biomass burning emissions occur after the harvest in autumn. In addition, given that amines are emitted from various industrial operations, such as chemical and leather manufacturing (Ge et al., 2011), the large industrial region to the south of Beijing could also have been an important source of NOA.

The COA was a common OA component in both summer and autumn. It was identified by a special spectrum and a unique diurnal pattern. The contribution of m/z 41 (mainly $C_3H_5^+$) and m/z 55 (mainly $C_4H_7^+$) in the COA MS were very, indicating a high percentage of unsaturated organic compounds (Figs. 4b and 6d), very close to the MS measured for primary Chinese cooking emissions by He et al. (2010). As shown in Figs. 5b and 7d, a good correlation was observed between the COA and the fragments of $C_6H_{10}O^+$, the main component of the COA MS: the correlation coefficients R^2 were 0.70 and 0.78 in summer and autumn, respectively (Sun et al., 2011). A clear and unique diurnal pattern of COA was observed, with two peaks at noon and in the evening, corresponding to the lunch and evening meal times of the local residents (Fig. 8a). However, the evening peak was much higher than the noon peak in autumn, consistent with the total OA trend. This indicates that the COA is an important OA component that determines the diurnal variation of OA. In addition, it was interesting to find a small peak corresponding to breakfast time on autumn mornings. This phenomenon was also observed by Sun et al. (2013). How-

ever, it did not appear in summer. Perhaps residents choose not to cook breakfast in the summer due to the hot weather. The COA was a very stable OA component in both seasons, with similar contributions to total OA (23% and 26%). This proportion is the same as other results in Beijing, such as 24% in summer and 23% in winter (Huang et al., 2010; Zhang et al., 2014). However, this component was not identified in Shanghai or Shenzhen (He et al., 2011; Huang et al., 2012). Rational management of the culinary industry is very important for reducing the OA concentration in Beijing. This could include encouraging residents to use simple soot filter equipment, and for restaurants to use fuel with improved combustion efficiency.

The HOA component was mainly attributed to primary combustion sources, which displayed high signals of the ion series $C_nH^+_{2n+1}$ and $C_nH^+_{2n-1}$ from alkenes plus cycloalkanes (Ng et al., 2010). This is very similar to previously reported reference spectra of POA (primary OA) emitted due to combustion of gasoline and diesel (Schneider et al., 2006). This component was also identified during both summer and autumn campaigns, both having an H/C ratio of 1.66, and similar O/C ratios (0.14 and 0.18, respectively). The O/C value was consistent with the results in Beijing 2008 (0.17; Huang et al., 2010) and Mexico City (0.18; Aiken et al., 2009). In addition, HOA correlated well with combustion tracers, such as NO_x ($R^2 = 0.62$ and 0.55; Figs. 5c and 7e). HOA accounted for 22% and 10% of the total OA mass in summer and autumn (Fig. 8b). The diurnal patterns of HOA during the two seasons were similar, with a prominent peak in the morning around rush hour, and a second higher peak appearing at night (Fig. 8a). This diurnal cycle was consistent with the number of heavy duty and diesel trucks in Beijing (Han et al., 2009). According to traffic regulations, these kinds of vehicles are only allowed inside the city between 22:00 and 06:00. After comparing this period with the diurnal cycle of HOA, we found that the highest value of this OA factor was more likely driven by the emissions from these kinds of vehicles (Sun et al., 2013). This finding was consistent with the Beijing 2008 results of Huang et al. (2010) and with those of other urban locations, such as the Po Valley (Saarikoski et al., 2012) and Barcelona (Mohr et al., 2012). These findings together indicate that HOA is likely a surrogate for combustion POA.

3.3. *Back trajectory clustering analysis*

The Hybrid Single-Particle Lagrangian Integrated Trajectory (HYSPLIT) model was used to analyze the effect of air mass transport on the OA loading and components in Beijing. The analysis steps were similar to those in Huang et al. (2010). First, 48-h back trajectories, starting at 500 m above ground level in Beijing (39.97°N, 116.37°E), were calculated every 6 h (at 0000, 0600, 1200 and 1800 LST) during the two seasons. The back trajectories (BTs) were then clustered according to their similarity in spatial distribution using HYSPLIT4 software (Draxler et al., 2009). As a result, a four-cluster and a three-cluster solution were suggested as the optimum clustering solution for summer and autumn (Fig. 9).

There was a significant difference in the BTs in summer and autumn. Almost all air masses in autumn came from western China. The origin of the air masses, however, was more complex in summer, and they were uniformly distributed around Beijing. The most frequently observed air mass was the fourth cluster in summer (at a frequency of

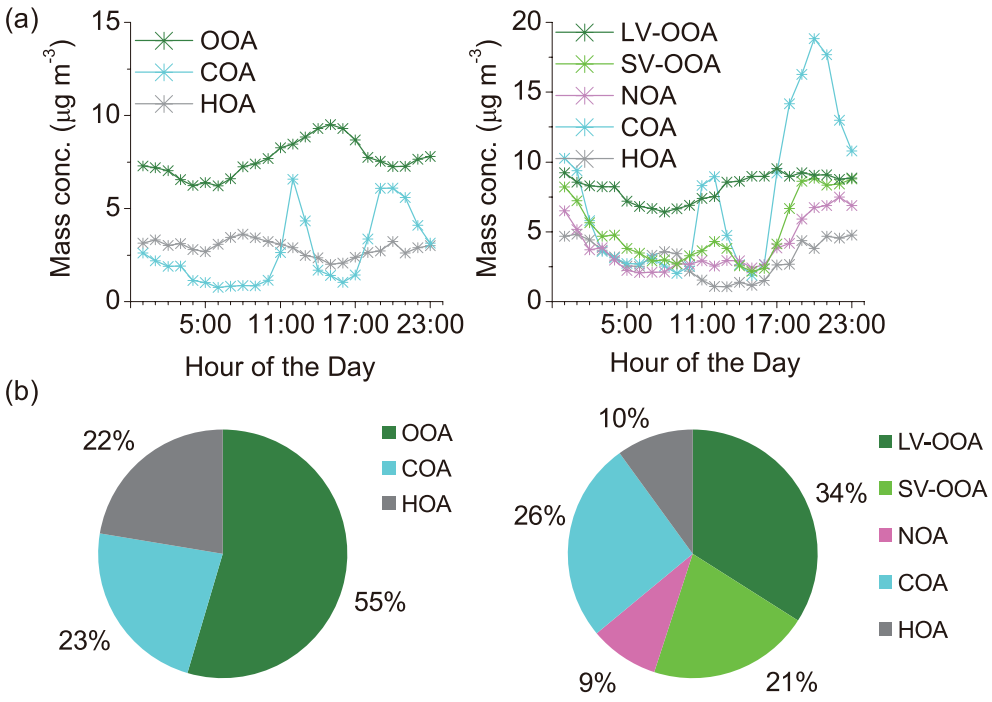

Fig. 8. (a) Diurnal variations of the OA components and (b) the average OA compositions in summer and autumn as pie charts.

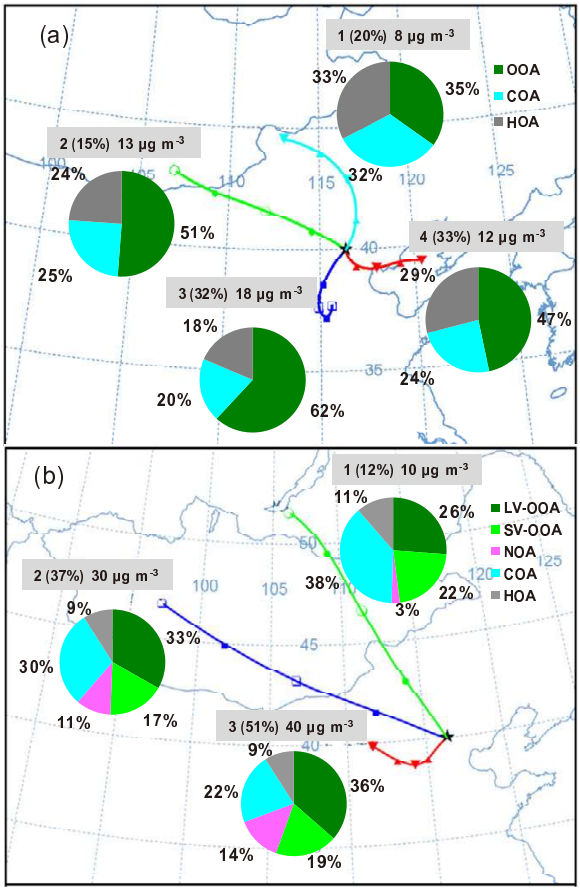

Fig. 9. Back trajectory groups, and the corresponding mean OA compositions as pie charts, during (a) summer and (b) autumn.

33%), which originated in the Bohai Sea region east of Beijing, and passed Tianjin, a large industrial city in northern China, before arriving. The highest OA loading appeared in the third cluster, which originated in Shandong Province and passed over Hebei province, and the cities of Jinan, Liaocheng, and Hengshui. Therefore, the air masses in this cluster could have carried pollutants from these cities, aggravating the pollution in Beijing. However, the most frequently observed air mass in autumn was the third cluster (at a frequency of 51%), which originated from the west and moved southeast at the start of the 12 hour period, after which it turned northeast and finally reached Beijing. This air mass passed over Shanxi and Hebei provinces, the largest coal-producing and consuming provinces in China, respectively. Unsurprisingly, the highest OA loading (40 μg m^{-3}) was observed in this cluster. The lowest OA loadings in the two seasons were similar and all observed in air masses originating north of Beijing; the corresponding concentrations were 8 and 10 μg m^{-3} in summer and autumn, respectively.

The contribution of each OA component was different in each cluster. The OA in the first clean cluster in both seasons was composed of the highest fraction of POA, such as HOA and COA. Their total contributions were 65% and 49% in summer and autumn, respectively, indicating a significant contribution of primary emissions in and around the vicinity of Beijing to aerosol pollution. The OA in the highest OA loading clusters (the third cluster 3 of both seasons) had the highest fractions of secondary aerosol. The contributions of OOA were 62% and 55% in summer and autumn, respectively. The heavy pollution cluster was associated with the geographical features of urban Beijing: generally flat and surrounded by mountains on all sides except the south.

As can be seen from the above analysis, the high OA concentration was associated with southerly air masses containing secondary regional pollutants; in contrast, the contribution of local, primary aerosol emissions were more important in northerly air masses, and the OA loading was much lower than that in the southerly air masses.

3.4. *OA component variations in different periods*

The observation in autumn not only included weekdays and weekends but also one of the most important festivals in China, the National Day of China, on 1 October. People's routines are different among these three periods, resulting in significant OA source changes. Therefore, studying the OA component changes during these three periods can reveal the effect of human activities on the ambient OA. Most residents' weekday activities follow a go-to-work–go-home pattern. Most office workers have no need to attend at weekends, so the rush disappears. During the National Day period, people have a 7 day holiday (from 1 to 7 October). Many residents leave Beijing, while many people come from elsewhere to visit the city.

The diurnal variations of SV-OOA and COA were similar during these three periods (Figs. 10b and d). The two COA peaks were lower during the National Day holiday period than on weekdays and weekends, because the OA emissions from family dining events were significantly reduced (most Beijing residents were traveling to other locations, even though a large number of tourists from other locations traveled to Beijing). This difference can be explained as follows: there are no primary filtering measures used in traditional family home cooking, whereas most large restaurants, where tourists dine, have installed advanced filtration equipment. Therefore, the emissions and the contribution of COA to the OA total during the National Day holiday period decreased (Fig. 10d). The diurnal variations of the other three OA components were different among the three periods (Figs. 10a, c and e). The greatest difference was observed for HOA, which presented a prominent peak in the morning around rush hour. Meanwhile, the weekday HOA morning peak was significantly higher than on weekends and the National Day holiday period. This appears consistent with the reduced morning rush hour on weekends and the holiday. In addition, the contribution of HOA to OA on weekdays was significantly higher than during the other two periods (Fig. 10f). This is consistent with the result measured by Rattigan et al. (2010) in New York. They found that the direct emissions from fossil fuel combustion were lower at weekends (approximately 27% and 38% lower on Saturday and Sunday, respectively) than on weekdays.

From the above analysis, it is clear that the primary or-

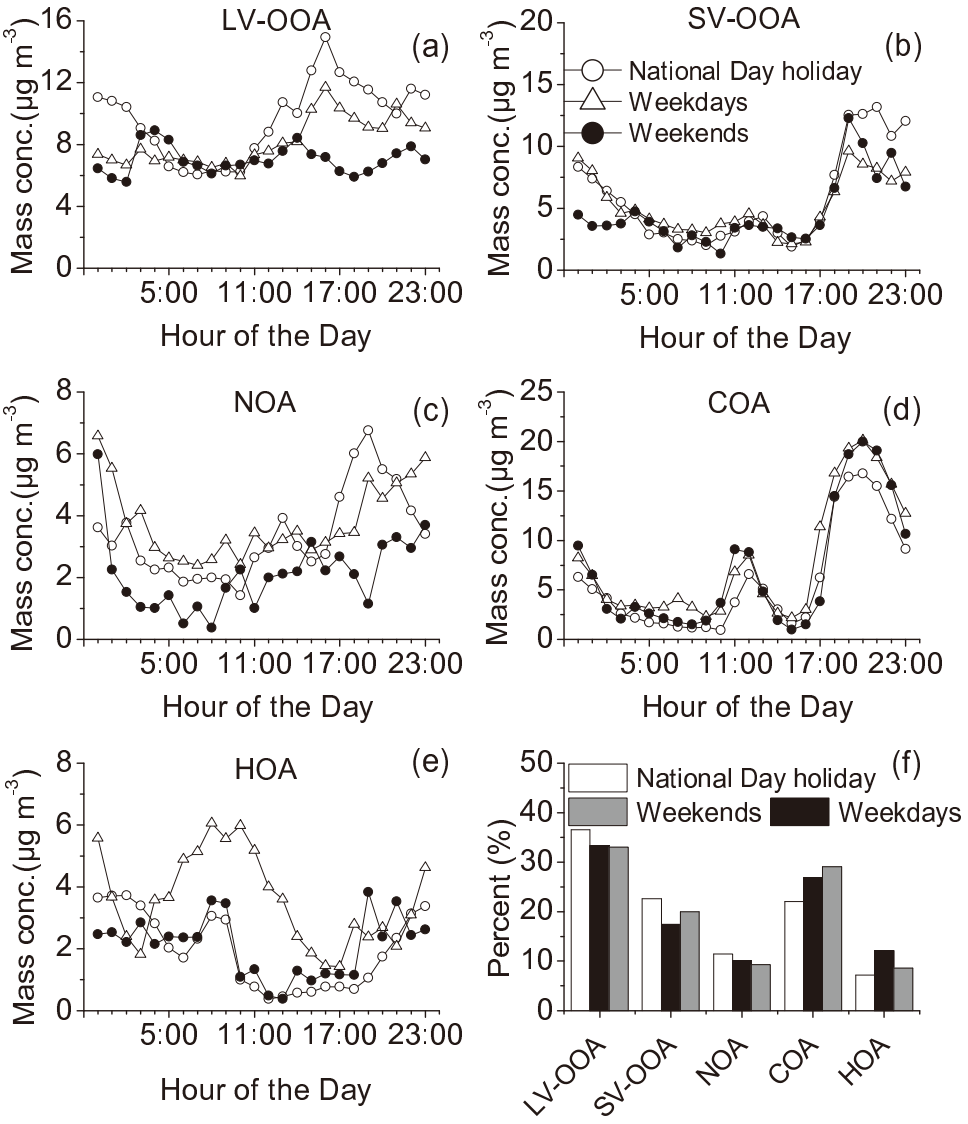

Fig. 10. The (a–e) diurnal variations and (f) percentage contributions of the different OA components on National Day holiday, weekdays and weekends.

ganic aerosols, HOA and COA, decreased during the National Day holiday period, and HOA decreased at the weekends compared with weekdays. It should be noted that we do not discuss the other three OA components in detail because the formation processes of these components are complicated and determined not only by the primary emission sources, but also by atmospheric conditions, such as anthropogenic influences, sunlight, atmospheric oxidation and regional transport. Therefore, this section is intended as a preliminary study on the effect of human activities on the POA component. Further and more in-depth studies, especially the effect on SOA, will require more observations and meteorological data.

4. Conclusions

Size-resolved OA was measured *in situ* using an HR-ToF-AMS during August and October 2012 in Beijing. The mean mass concentrations of OA in summer and autumn were 13 ± 6.9 μg m^{-3} and 30 ± 30 μg m^{-3}, respectively. The OA showed a very different trend in the two seasons, which was more stable in summer than autumn. The average OA size distribution in the two seasons was similar and spanned a broad range, with the appearance of the highest peak at ∼600 nm and another small peak at ∼200 nm. The diurnal variations of OA displayed two broad peaks, one at noon and the other in the evening, mainly affected by the COA component. Meanwhile, the concentration difference of the two peaks was higher in autumn, possibly caused by differences in meteorological factors. The elemental analysis found that the ratios of O/C and OM/OC were all higher in summer. Therefore, the OA was more aged in the warmer season. PMF analysis indicated three and five OA components for summer and autumn, and that the OOA accounted for about 55% of the total OA. Back trajectory clustering analysis indicated that the southerly air mass was associated with the highest OA loading, and was rich in oxidized organic species. How-

ever, OA in northern air masses contained a large fraction of primary HOA and COA species. There was a significant effect of human activities on the OA components, especially during the long National Day holiday, when the COA and HOA levels obviously decreased.

Acknowledgements. This study was supported by the "Strategic Priority Research Program" of the Chinese Academy of Sciences (Grant No. XDA05100100&XDB05020000) and the National Natural Science Foundation of China (Grant Nos. 41230642 & 41275139).

Electronic Supplementary Material: Supplementary material [(1) the location of the monitoring site; (2) the discussions about choosing the CE value and PMF solution; (3) the time series of meteorological factors in summer and autumn)] is available online at http://dx.doi.org/10.1007/s00376-014-4153-9.

REFERENCES

Aiken, A. C., and Coauthors, 2009: Mexico City aerosol analysis during MILAGRO using high resolution aerosol mass spectrometry at the urban supersite (T0)—Part 1: Fine particle composition and organic source apportionment. *Atmospheric Chemistry and Physics*, **9**, 6633–6653.

Alam, K., T. Trautmann, and T. Blaschke, 2011: Aerosol optical properties and radiative forcing over mega-city Karachi. *Atmospheric Research*, **101**, 773–782.

Asa-Awuku, A., M. A. Miracolo, J. H. Kroll, A. L. Robinson, and N. M. Donahue, 2009: Mixing and phase partitioning of primary and secondary organic aerosols. *Geophys. Res. Lett.*, **36**, L15827, doi: 10.1029/2009GL039301.

Canagaratna, M. R., and Coauthors, 2007: Chemical and microphysical characterization of ambient aerosols with the aerodyne aerosol mass spectrometer. *Mass Spectrometry Reviews*, **26**, 185–222.

Crippa, M., and Coauthors, 2013: Identification of marine and continental aerosol sources in Paris using high resolution aerosol mass spectrometry. *J. Geophys. Res.: Atmos.*, **118**, 1950–1963, 10.1002/jgrd.50151.

DeCarlo, P. F., and Coauthors, 2006: Field-deployable, high-resolution, time-of-flight aerosol mass spectrometer. *Analytical Chemistry*, **78**, 8281–8289.

Draxler, R., B. Stunder, G. Rolph, A. Stein, and A. Taylor, 2009: HYSPLIT4 user's guide. Version 4.9, NOAA Air Resour. Lab., Silver Spring, Md. [Available online at http://ready.arl.noaa. gov/HYSPLIT.php.]

Drewnick, F., and Coauthors, 2005: A new Time-of-Flight Aerosol Mass Spectrometer (TOF-AMS)-instrument description and first field deployment. *Aerosol Science and Technology*, **39**, 637–658.

Ge, X. L., A. S. Wexler, and S. L. Clegg, 2011: Atmospheric amines—Part I. A review. *Atmos. Environ.*, **45**, 524–546.

Han, S., and Coauthors, 2009: Temporal variations of elemental carbon in Beijing. *J. Geophys. Res.*, **114**, D23202, doi: 10.21029/22009JD012027.

He, L. Y., X. F. Huang, L. Xue, M. Hu, Y. Lin, J. Zheng, R. Zhang, and Y. H. Zhang, 2011: Submicron aerosol analysis and organic source apportionment in an urban atmosphere in Pearl River Delta of China using high-resolution aerosol mass spectrometry. *J. Geophys. Res.*, **116**, D12304, doi: 10.1029/2010JD014566.

He, L. Y., M. Hu, X. F. Huang, Y. H. Zhang, and X. Y. Tang, 2006: Seasonal pollution characteristics of organic compounds in atmospheric fine particles in Beijing. *The Science of the Total Environment*, **359**, 167–176.

He, L. Y., and Coauthors, 2010: Characterization of high-resolution aerosol mass spectra of primary organic aerosol emissions from Chinese cooking and biomass burning. *Atmospheric Chemistry and Physics*, **10**, 11535–11543.

He, Q. S., and J. T. Mao, 2005: Observation of urban mixed layer at Beijing using a micro pulse lidar. *Acta Meteorologica Sinica*, **63**, 374–384. (in Chinese)

Huang, X. F., and Coauthors, 2011: Characterization of submicron aerosols at a rural site in Pearl River Delta of China using an Aerodyne High-Resolution Aerosol Mass Spectrometer. *Atmospheric Chemistry and Physics*, **11**, 1865–1877.

Huang, X. F., and Coauthors, 2010: Highly time-resolved chemical characterization of atmospheric submicron particles during 2008 Beijing Olympic Games using an Aerodyne High-Resolution Aerosol Mass Spectrometer. *Atmospheric Chemistry and Physics*, **10**, 8933–8945.

Huang, X. F., L. Y. He, L. Xue, T. L. Sun, L. W. Zeng, Z. H. Gong, M. Hu, and T. Zhu, 2012: Highly time-resolved chemical characterization of atmospheric fine particles during 2010 Shanghai World Expo. *Atmospheric Chemistry and Physics*, **12**, 4897–4907.

Jimenez, J. L., and Coauthors, 2003: Ambient aerosol sampling using the Aerodyne Aerosol Mass Spectrometer. *J. Geophys. Res.: Atmos.*, **108**, 8425, doi: 10.1029/2001JD001213.

Jimenez, J. L., and Coauthors, 2009: Evolution of organic aerosols in the atmosphere. *Science*, **326**, 1525–1529.

Lanz, V. A., M. R. Alfarra, U. Baltensperger, B. Buchmann, C. Hueglin, and A. S. H. Prévôt, 2007: Source apportionment of submicron organic aerosols at an urban site by factor analytical modelling of aerosol mass spectra. *Atmospheric Chemistry and Physics*, **7**, 1503–1522.

Lan, Z. J., D. L. Chen, X. Li, X. F. Huang, L. Y. He, Y. G. Deng, N. Feng, M. Hu, 2011: Modal characteristics of carbonaceous aerosol size distribution in an urban atmosphere of South China. *Atmospheric Research*, **100**, 51–60.

Mohr, C., and Coauthors, 2012: Identification and quantification of organic aerosol from cooking and other sources in Barcelona using aerosol mass spectrometer data. *Atmospheric Chemistry and Physics*, **12**, 1649–1665.

Ng, N. L., and Coauthors, 2010: Organic aerosol components observed in Northern Hemispheric datasets from Aerosol Mass Spectrometry. *Atmospheric Chemistry and Physics*, **10**, 4625–4641.

Pang, Y., B. J. Turpin, and L. A. Gundel, 2006: On the importance of organic oxygen for understanding organic aerosol particles. *Aerosol Science and Technology*, **40**, 128–133.

Paatero, P., and U. Tapper, 1994: Positive matrix factorization: A nonnegative factor model with optimal utilization of error estimates of data values. *Environmetrics*, **5**, 111–126.

Paatero, P., and P. K. Hopke, 2003: Discarding or downweighting highnoise variables in factor analytic models. *Analytica Chimica Acta*, **490**, 277–289.

Rattigan, O. V., H. D. Felton, M. S. Bae, J. J. Schwab, and K. L. Demerjian, 2010: Multi-year hourly $PM_{2.5}$ carbon measurements in New York: Dirunal, day of week and seasonal patterns. *Atmos. Environ.*, **44**, 2043–2053.

Saarikoski, S., and Coauthors, 2012: Chemical characterization of springtime submicrometer aerosol in Po Valley, Italy. *Atmospheric Chemistry and Physics*, **12**, 8401–8421.

Schneider, J., and Coauthors, 2006: Mass spectrometric analysis and aerodynamic properties of various types of combustion-related aerosol particles. *International Journal of Mass Spectrometry*, **258**, 37–49.

Sun, J., and Coauthors, 2010: Highly time-and size-resolved characterization of submicron aerosol particles in Beijing using an Aerodyne Aerosol Mass Spectrometer. *Atmospheric Environment*, **44**, 131–140.

Sun, Y. L., and Coauthors, 2011: Characterization of the sources and processes of organic and inorganic aerosols in New York city with a high-resolution time-of-flight aerosol mass apectrometer. *Atmospheric Chemistry and Physics*, **11**, 1581–1602.

Sun, Y. L., Z. F. Wang, P. Q. Fu, T. Yang, Q. Jiang, H. B. Dong, J. Li, and J. J. Jia, 2013: Aerosol composition, sources and processes during wintertime in Beijing, China. *Atmospheric Chemistry and Physics*, **13**, 4577–4592.

Ulbrich, I. M., M. R. Canagaratna, Q. Zhang, D. R. Worsnop, and J. L. Jimenez, 2009: Interpretation of organic components from positive matrix factorization of aerosol mass spectrometric data. *Atmospheric Chemistry and Physics*, **9**, 2891–2918.

Ulbrich, I. M., M. R. Canagaratna, M. J. Cubison, Q. Zhang, N. L. Ng, A. C. Aiken, and J. L. Jimenez, 2012: Three-dimensional factorization of size-resolved organic aerosol mass spectra from Mexico City. *Atmospheric Measurement Techniques*, **5**, 195–224.

You, H. L., W. D. Liu, and J. R. Tan, 2010: Temporal characteristics of atmospheric maximum mixing depth of Beijing. *Meteorological Monthly*, **36**, 51–55. (in Chinese)

Yu, X. N., B. Zhu, Y. Yin, J. Yang, Y. W. Li, and X. L. Bu, 2011: A comparative analysis of aerosol properties in dust and haze-fog days in a Chinese urban region. *Atmospheric Research*, **99**, 241–247.

Zhang, J. K., Y. Sun, Z. R. Liu, D. S. Ji, B. Hu, Q. Liu, and Y. S. Wang, 2014: Characterization of submicron aerosols during a month of serious pollution in Beijing, 2013. *Atmospheric Chemistry and Physics*, **14**, 2887–2903.

Zhang, Q., M. R. Canagaratna, J. T. Jayne, D. R. Worsnop, and J. L. Jimenez, 2005a: Time-and size-resolved chemical composition of submicron particles in Pittsburgh: Implications for aerosol sources and processes. *J. Geophys. Res.*, **110**, D07S09, doi: 10.1029/2004JD004649.

Zhang, Q., D. R. Worsnop, M. R. Canagaratna, and J. L. Jimenez, 2005b: Hydrocarbon-like and oxygenated organic aerosols in Pittsburgh: insights into sources and processes of organic aerosols. *Atmospheric Chemistry and Physics*, **5**, 8421–8471.

Zhang, Q., and Coauthors, 2007: Ubiquity and dominance of oxygenated species in organic aerosols in anthropogenically-influenced Northern Hemisphere midlatitudes. *Geophys. Res. Lett.*, **34**, L13801, doi: 10.1029/2007GL029979.

Zhang, Q., J. L. Jimenez, M. R. Canagaratna, I. M. Ulbrich, N. L. Ng, D. R. Worsnop, and Y. L. Sun, 2011: Understanding atmospheric organic aerosols via factor analysis of aerosol mass spectrometry: A review. *Analytical and Bioanalytical Chemistry*, **401**, 3045–3067.

Zhang, Y. M., J. Y. Sun, X. Y. Zhang, X. J. Shen, T. T. Wang, and M. K. Qin, 2013: Seasonal characterization of components and size distributions for submicron aerosols in Beijing. *Science in China: Earth Sciences*, **56**(5), 890–900, doi: 10.1007/s11430-012-4515-z.